Materials and Design 54 (2014) 967–972

Contents lists available at ScienceDirect

Materials and Design

journal homepage: www.elsevier.com/locate/matdes

Hydrogen-induced hardening of Ti–6Al–4V alloy in β phase field

Jingwei Zhao [a,*], Hua Ding [b], Zhengyi Jiang [a], Mingli Huang [b], Hongliang Hou [c]

[a] School of Mechanical, Materials and Mechatronic Engineering, University of Wollongong, NSW 2522, Australia
[b] School of Materials and Metallurgy, Northeastern University, Shenyang 110004, PR China
[c] Beijing Aeronautical Manufacturing Technology Research Institute, Beijing 100024, PR China

ARTICLE INFO

Article history:
Received 28 April 2013
Accepted 14 September 2013
Available online 21 September 2013

Keywords:
Ti–6Al–4V alloy
Hydrogen
Hot deformation
Hardening

ABSTRACT

Isothermal compression tests were conducted to investigate the hot deformation behaviour of a Ti–6Al–4V alloy with different hydrogen contents (0, 0.35 and 0.6 wt.%) at temperatures of 1050–1100 °C, and strain rates of 0.005, 0.01, 0.1 and 1 s^{-1} respectively. The microstructural evolution was investigated via optical microscope (OM), X-ray diffraction (XRD) and transmission electron microscope (TEM). The mechanism of hydrogen-induced hardening was discussed. The experimental results showed that hydrogen could be retained in Ti–6Al–4V alloy even though the temperature was increased to 1100 °C in air. δ hydride with an face-centred cubic (FCC) crystal structure existed in the deformed matrix, and the size of δ hydride reduced when the deformation temperature was increased from 1050 to 1100 °C. Hydrogen induced the increased flow stress and work hardening rate of Ti–6Al–4V alloy when deformed in β phase field. Hydrogen had a positive effect on the development of twinning in Ti–6Al–4V alloy. Based on the analysis of both hot deformation behaviour and microstructural evolution, it is indicated that the hydrogen-induced twinning plays a key role in the enhancement of work hardening of Ti–6Al–4V alloy in β phase field.

1. Introduction

Ti–6Al–4V alloy is a (α + β) dual-phase titanium alloy and has been widely used in the aerospace and biomaterials industries due to its advantageous combination of properties like high specific strength, excellent resistance to environmental degradation, low modulus of elasticity, high resistance to impact loading and low coefficient of thermal expansion [1]. In general, the microstructure and mechanical properties of titanium alloys are extremely sensitive to the hot processing parameters. In order to acquire the desired mechanical properties, numerous investigations have been conducted on the deformation stability, flow behaviour and cavity formation of Ti–6Al–4V alloy during hot working by physical and mathematical simulative techniques [2–5]. Ti–6Al–4V alloy is, however, more difficult to fabricate relative to other metallic materials by conventional hot working processes owing to its poor formability. Even though hot deformation in practical industrial processes such as hot forging, rolling or extrusion has been extensively used for the manufacturing of both semi-finished and finished products of Ti–6Al–4V alloy, the application of Ti–6Al–4V alloy is still restricted because of the complicated manufacturing processes and high production cost [6].

To improve the formability of Ti–6Al–4V alloy during hot working, thermo hydrogen treatment (THT) technique has been suggested by many researchers. Shan et al. [7] studied the flow behaviour of Ti–6Al–4V–H alloy in the temperature range of 750–980 °C. They found that the flow stress decreased with an increase of the hydrogen content in the (α + β) dual-phase range due to the hydrogen-induced flow softening of α phase and an increase in the volume fraction of the softer β phase. The work of Zhang and Zhao [8] showed that the addition of a small amount of hydrogen into Ti–6Al–4V alloy improved the superplasticity, decreased the dislocation density and promoted the flow of β phase along α–α grain boundaries. The lowest deformation temperature and smallest unstable region could be obtained in the isothermal compression of Ti–6Al–4V alloy with a hydrogen content of 0.4 wt% [9]. Lu et al. [10] indicated that the addition of hydrogen in Ti–6Al–4V alloy induced enhanced superplastic elongation, increased optimum superplastic strain rate and decreased optimum superplastic deformation temperature. The aforementioned studies mainly focused on the effects of hydrogen on the deformation behaviour of Ti–6Al–4V alloy in the (α + β) dual-phase range. Typically, thermomechanical processing of the ingot of Ti–6Al–4V alloy comprises β hot working and β annealing to refine/recrystallise the β grain structure followed by (α + β) hot working to break down the transformed microstructure produced during cooling from the β phase field [5,11]. Bulk metalworking of Ti–6Al–4V alloy generally involves a series of mechanical processing steps, including

* Corresponding author. Tel.: +61 2 42214774; fax: +61 2 42215474.
E-mail addresses: jwzhaocn@gmail.com (J. Zhao), hding@263.net (H. Ding), jiang@uow.edu.au (Z. Jiang).

0261-3069/$ - see front matter
http://dx.doi.org/10.1016/j.matdes.2013.09.035

upsetting/side pressing, cogging or extrusion at temperatures above the (α + β)/β phase transition temperatures [12]. Besides (α + β) dual-phase field, investigation on the deformation behaviour in the β phase field is thus essential in order to obtain valuable reference for hot working of such alloy. However, the effect of hydrogen on the deformation behaviour of Ti–6Al–4V alloy in the β phase field has been less investigated extensively.

Senkov and Jonas [13] studied the hot deformation behaviour of titanium-hydrogen alloys in air over the temperature range from 500 to 1000 °C within the α, (α + β) and β phases fields, and found that hydrogen could be retained at temperatures up to 980 °C due to the formation of an oxidised film on the specimen surface. The (α + β)/β phase transition temperature of Ti–6Al–4V alloy is about 990 °C. When deformed in the β phase field (above 990 °C), hydrogen will escape from the tested Ti–6Al–4V alloy based on the work of Senkov and Jonas [13]. Previous investigations have shown that the hot workability and flow stress of β titanium alloys decreases and increases, respectively, after hydrogenation, and the mechanism of hydrogen-induced hardening of β titanium alloys has been well studied [14,15]. The hardening behaviour of hydrogenated Ti–6Al–4V alloy that deformed in β phase field, however, has not been well reported, and the mechanism for this alloy is still not understood. In particular, there is still a lack of detailed research on whether the hydrogen can be well retained in the Ti–6Al–4V alloy when it is deformed in β phase field.

This study is to investigate the hot deformation behaviour and microstructural evolution of hydrogenated Ti–6Al–4V alloys in β phase field. Detailed research is conducted to determine whether the hydrogen can be retained in the specimens during hot deformation. The hardening behaviour of the hydrogenated Ti–6Al–4V alloy in β phase field is analysed, and the mechanism of hydrogen-induced hardening is discussed.

2. Experimental procedure

The material used was a Ti–6Al–4V alloy, the (α + β)/β phase transition temperature of which is about 990 °C. The microstructure of the as-received Ti–6Al–4V alloy comprises of polygonal α (bright) and β (grey) phases, as shown in Fig. 1. Cylindrical specimens with diameter of 10 mm and height of 15 mm were prepared according to ASTM: E209. The specimens were hydrogenated at 750 °C by holding them in a pure hydrogen environment for 2 h followed by air-cooling to room temperature. Specimens with various hydrogen contents (0, 0.35 and 0.6 wt.%) were obtained by controlling the hydrogen pressure, and the actual hydrogen content was determined by weighing the specimen before and after hydrogenation.

Isothermal hot compression tests were conducted on a Gleeble-1500D thermo-mechanical simulator in air with strain rates of 0.005, 0.01, 0.1 and 1 s^{-1} respectively at temperatures of 1050–1100 °C to investigate the hot deformation behaviour of Ti–6Al–4V alloy with different hydrogen contents. In order to minimise friction and barrel development during deformation, and to prevent bonding of the specimens to the anvils, graphitic lubricant was applied to the mating surfaces. The specimens were heated to the deformation temperatures at a rate of 10 °C/s, then held for 3 min, and finally compressed with a maximum height reduction of 50%. The tested specimens were immediately quenched in water after deformation. The schedule for isothermal hot compression tests is schematically shown in Fig. 2.

Metallographic specimens were etched with a "9 vol.% hydrofluoric acid + 27 vol.% nitric acid + 64 vol.% water" solution for microstructural observation by an OLYMPUS GX51 optical microscope (OM). Phase constituents were measured by X-ray diffraction (XRD) using Cu Kα radiation at 40 kV and 40 mA. Disc samples with a diameter of 3 mm, which were cut perpendicular to the compression direction, were used for transmission electron microscope (TEM) investigations. The TEM samples were prepared by electro-polishing in an electrolyte of "6 vol.% $HClO_4$ + 34 vol.% C_4H_9OH + 60 vol.% CH_3OH" with temperature of −40 to −35 °C, voltage of 50–55 V and current of 30–35 mA. TEM observations were carried out on a TECNAL G^2 20 microscope operated at 200 kV.

3. Results and discussion

3.1. Phase identification before hot deformation

Fig. 3 shows the XRD patterns of the 0H, 0.35H and 0.6H specimens (Ti–6Al–4V specimens with 0, 0.35% and 0.6 wt.% hydrogen, respectively) before hot deformation. In Fig. 3, α′ is the hexagonal martensite, and δ is the face-centred cubic (FCC, *a* = 0.444 nm) titanium hydride. The determination of α′ and δ has been detailed in our previous work [16]. It can be seen that the relative intensity of β phase diffraction peaks increases with an increase of the hydrogen content. The peaks of α′ and δ appear in the hydrogenated specimens, indicating α′ and δ were formed when the alloy was hydrogenated at 750 °C for 1 h followed by air-cooling to room temperature. In addition, the β peaks move to lower angles gradually with the increase of hydrogen content. β phase, a body-centred cubic (BCC) structure, consists of 12 tetrahedral interstices and 6 octahedron interstices. After hydrogenation, hydrogen atoms occupy the interstitial sites of β unit cell, and thus expand the lattice spacing which leading to the reduction of Bragg diffraction angle [17]. In contrast, there are only 4 tetrahedral interstices and 2

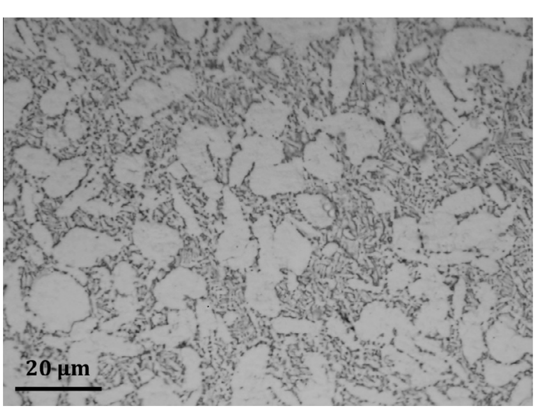

Fig. 1. Microstructure of the as-received Ti–6Al–4V alloy.

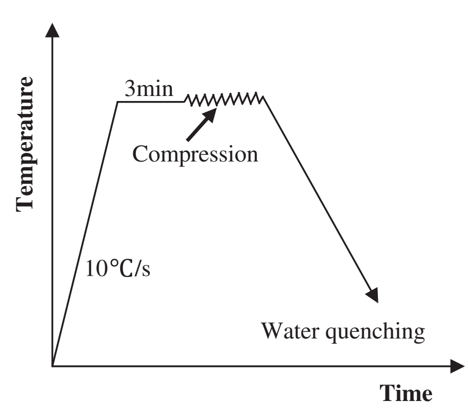

Fig. 2. Schematic illustration of the schedule for isothermal hot compression tests.

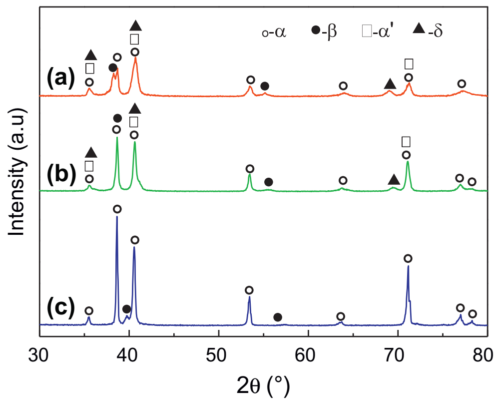

Fig. 3. XRD patterns of the (a) 0H, (b) 0.35H and (c) 0.6H specimens before hot deformation.

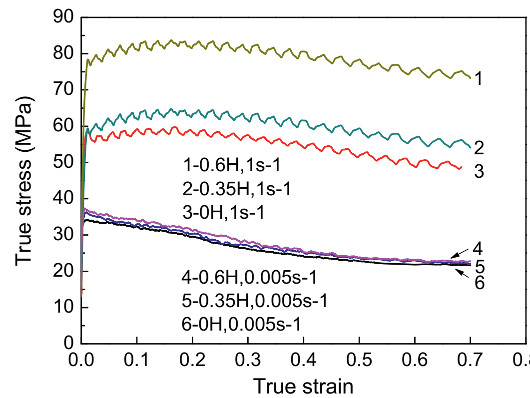

Fig. 5. Typical flow stress curves of the 0H, 0.35H and 0.6H specimens deformed at 1050 °C with different strain rates.

octahedron interstices in α (close-packed hexagonal, HCP) structure, and the solubility of hydrogen in α phase is far less than that in β phase, no significant moving of the α phase diffraction peaks is therefore found as the hydrogen content is increased.

3.2. Hydride characterisation after hot deformation

Fig. 4 shows the TEM micrographs of δ hydrides observed in the deformed 0.35H specimens. It can be seen that δ hydrides exist in the specimens that deformed at both 1050 °C and 1100 °C, indicating hydrogen could be retained in the Ti–6Al–4V alloy even though the temperature was increased to 1100 °C in air. Bulk hydrides are found in the specimen that deformed at 1050 °C, as shown in Fig. 4a. With increasing the temperature from 1050 to 1100 °C, the hydrides are needle-like, as shown in Fig. 4c. The hydrides present different characterisations when the specimens are deformed at different temperatures, and the size of hydrides is fine at 1100 °C in contrast to that at 1050 °C. When the temperature is increased, the stabilisation of the oxidised film on the specimen surface decreases [13]. The refining of δ hydride at 1100 °C relative to that at 1050 °C should be attributed to the reduction of the amount of hydrogen in the specimen due to the escape of some hydrogen when the temperature is increased.

3.3. Hardening behaviour

The typical flow stress curves of the 0H, 0.35H and 0.6H specimens are shown in Fig. 5. Oscillated flat flow curves are found at the strain rate of 1 s^{-1}, and continuous flow softening after a peak stress is observed at the strain rate of 0.005 s^{-1}. Oscillations indicate the possibility of localised or unstable plastic flow during hot deformation [12], and the flat flow curves are indicative of steady state flow behaviour. Flow softening of Ti–6Al–4V alloy during isothermal hot compression is known to occur due to the deformation heating and microstructural evolution such as dynamic recrystallisation (DRX) and dynamic globularisation [18]. In addition, the flow stress increases gradually with hydrogen at the strain rate of 1 s^{-1}. At the strain rate of 0.005 s^{-1}, however,

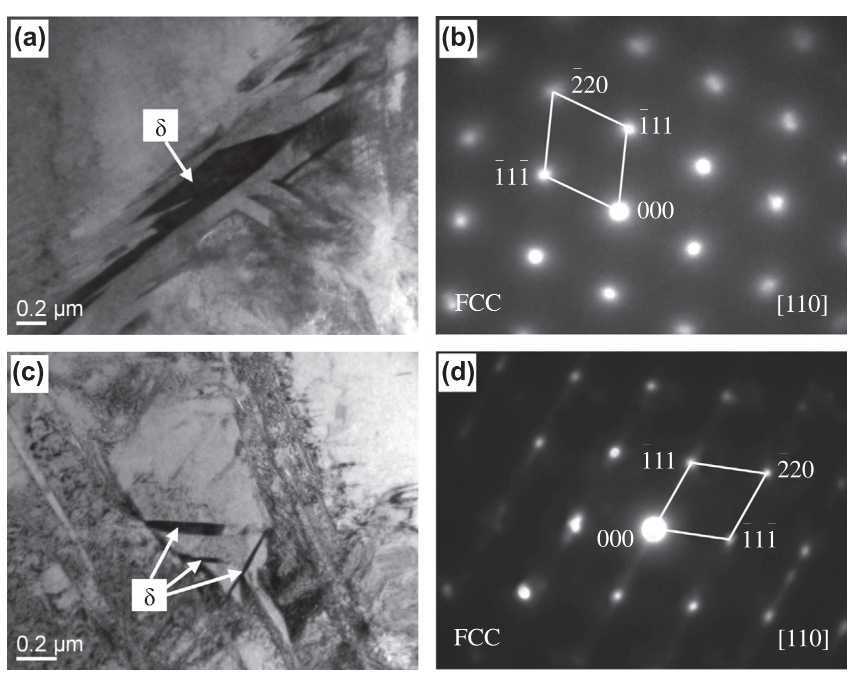

Fig. 4. TEM micrographs of δ hydrides observed in the 0.35H specimens deformed at (a and b) 1050 °C and (c and d) 1100 °C with strain rate of 1 s^{-1}. (a and c) δ hydrides and (b and d) SAED patterns.

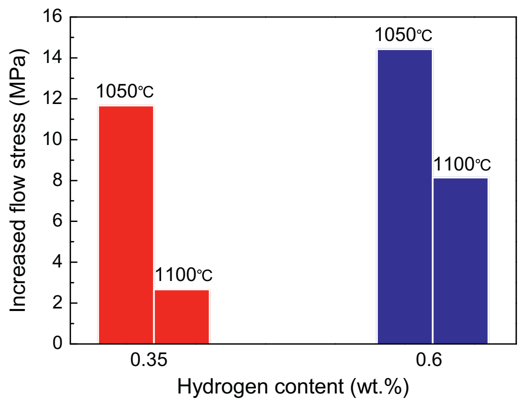

Fig. 6. Increased flow stress of Ti–6Al–4V alloy after 0.35% and 0.6% hydrogen additions at 1050 °C and 1100 °C with strain of 0.7 and strain rate of 0.1 s^{-1}.

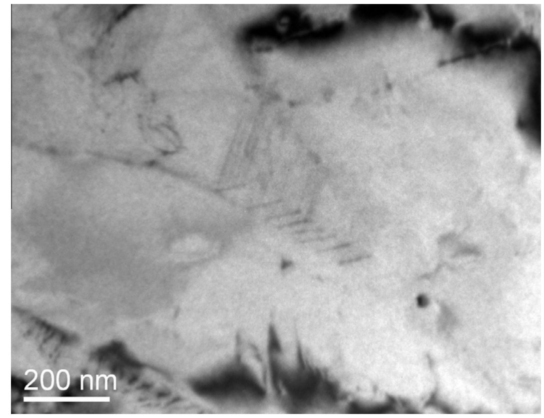

Fig. 9. TEM micrograph of dislocations observed in the 0.35H specimen deformed at 1050 °C with strain rate of 1 s^{-1}.

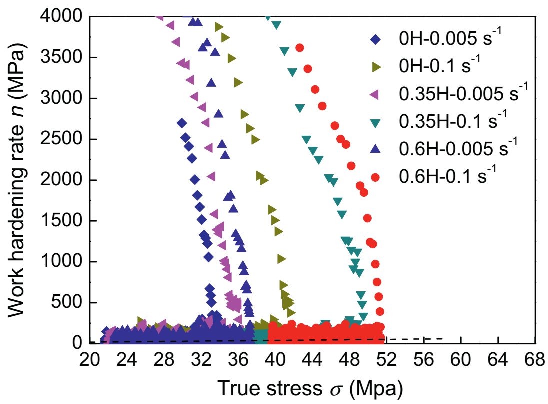

Fig. 7. Dependence of work hardening rate on true stress of the 0H, 0.35H and 0.6H specimens deformed at 1050 °C with different strain rates.

hydrogen shows little effect on the flow stress. With decreasing the strain rate from 1 to 0.005 s^{-1}, the time required for a hot deformation process is significantly increased. The failing of the effect of hydrogen on the flow stress at 0.005 s^{-1} relative to that at 1 s^{-1} is thought to be related to the massive loss of hydrogen from the specimen during the very slow deformation process in air.

Fig. 6 illustrates the increased flow stress of Ti–6Al–4V alloy after 0.35% and 0.6% hydrogen additions at 1050 °C and 1100 °C, respectively, relative to that without hydrogen. It can be seen that the increased flow stress at 1050 °C is higher than that at 1100 °C under the same hydrogen level. Additionally, after addition of 0.35% and 0.6% hydrogen in Ti–6Al–4V alloy, the increased flow stress values are 11.7 and 14.2 MPa at 1050 °C, and 2.7 and 8.2 MPa at 1100 °C, respectively. Hydrogen shows a reduced effect on the increment of flow stress at 1100 °C relative to that at 1050 °C, which is consistent with the TEM observations that less hydrogen is retained in the specimen at 1100 °C than that at 1050 °C.

Work hardening is an important feature of metals, and it is the strengthening of a metal induced by plastic deformation. Based on the Kocks–Mecking [19] approach, the work hardening behaviour of Ti–6Al–4V alloy at given hydrogen content, deformation temperature and strain rate can be described using the variations of instantaneous work hardening rate n ($n = d\sigma/d\varepsilon$, where σ is the true stress, and ε is the true strain) with σ. Fig. 7 shows the dependence of work hardening rate on the true stress of the 0H, 0.35H and 0.6H specimens. It can be seen that n–σ plots shift to high stresses with an increase of hydrogen content at a given strain rate, indicating the work hardening rate of Ti–6Al–4V alloy increased after hydrogenation. Moreover, the work hardening rate shows an increasing trend with the strain rate for the specimens with the same hydrogen content.

3.4. Mechanism of hydrogen-induced hardening

Fig. 8 shows the TEM micrographs of the 0H specimen after isothermal compression test where the micrographs are taken from the longitudinal section of the specimen with compression direction parallel to the vertical direction of the micrographs. As shown in Fig. 8a, localised flow occurs in the deformed 0H specimen, and gliding lines along the flow direction appear. Additionally, a large

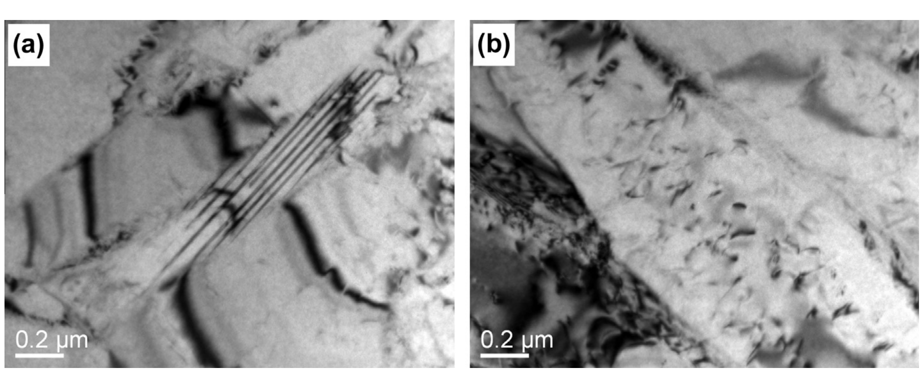

Fig. 8. TEM micrographs of the 0H specimen deformed at 1050 °C with strain rate of 1 s^{-1}: (a) localised flow and (b) dislocations.

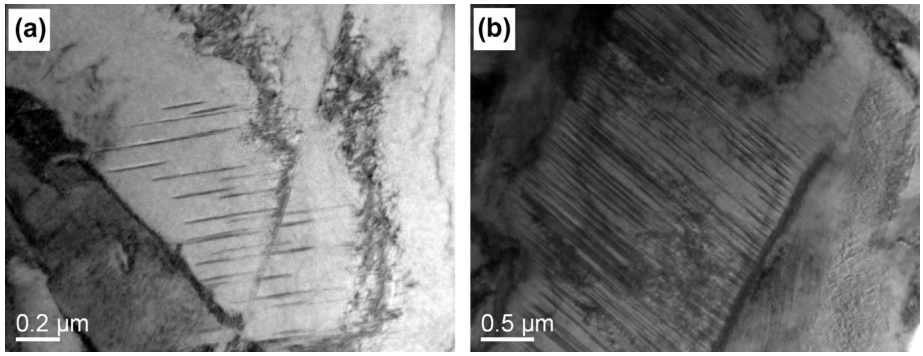

Fig. 10. TEM micrographs of twinning observed in the (a) 0.35H and (b) 0.6H specimens deformed at 1050 °C with strain rate of 1 s^{-1}.

number of dislocations are found in the deformed matrix, as shown in Fig. 8b. The thermal conductivity of titanium alloy is low relative to other metal alloys, and local temperature rising will occur during hot deformation [20]. When the strain rate is high (1 s^{-1} in this study), the flow localisation occurs easily and the level of flow instability increases due to the lack of enough time to homogenise the temperature and consume the accumulated dislocations of the specimen during hot deformation, leading to the appearance of localised flow and dislocations in the deformed matrix.

It has been reported that hydrogen in solution in titanium alloys lowers the strength of dislocation interactions with various obstacles, and the mobility of dislocations is enhanced [21]. In addition, the hydrogen in solution, being highly mobile and occupying interstitial sites near dislocations, prevents other solutes from segregating to the mobile dislocations [15]. Thus, a decreased number of dislocations in the deformed Ti–6Al–4V alloy are expected after hydrogenation. As shown in Fig. 9, the density of dislocations in the 0.35H specimen is low relative to that in the 0H specimen based on a large number of experimental results. The effect of dislocation density (ρ) on the flow stress (σ) is generally described as [22]:

$$\sigma = aG\boldsymbol{b}\rho^{1/2} \tag{1}$$

where G is the shear modulus, $\boldsymbol{b}$ is the Burgers vector, and the parameter a characterises both the strength and the statistical distribution of junction reactions. Obviously, the flow stress decreases with decreasing the dislocation density, indicating that the decreased dislocation density is not beneficial to the occurrence of hardening after hydrogenation. Another factor, twinning, is then considered to analyse the mechanism of hydrogen-induced hardening.

A lot of work has indicated that hydrogen induces decreased stacking fault energy (SFE) of BCC [23], TiAl [24,25], Ti40 [20] and Ti–6Al–4V [26] alloys during deformation. The work hardening characteristics of a metal are strongly influenced by the SFE [27]. Decrease of SFE favours the development of twinning, leading to hardening occurs easily during deformation process [28]. Fig. 10a and b present the TEM micrographs of twinning observed in the 0.35H and 0.6H specimens, respectively. A large number of twins appear in the hydrogenated specimens, while no twins are found in the 0H specimen, indicating that hydrogen has a positive effect on the proceeding of twinning in Ti–6Al–4V alloy. Therefore, hydrogen-induced twinning is considered to be the main reason for the enhancement of work hardening of Ti–6Al–4V alloy in the β phase field. Moreover, the density of twins in the 0.6H specimen is higher than that in the 0.35H specimen, and a further enhanced work hardening is expected. The increase of work hardening rate is closely related with the onset of deformation twinning in the compression test of titanium [29]. An increased work hardening rate will be obtained due to the generation of twinning in the matrix of Ti–6Al–4V alloy after hydrogenation during hot deformation, as shown in Fig. 7.

As regards the reasons for the hydrogen-induced hardening of Ti–6Al–4V alloy deformed in the β phase field, the following causes are considered. One is the solid solution strengthening after hydrogenation, which comes from the fact that the solubility of hydrogen in the β phase is far more than that in the α phase, and large numbers of hydrogen atoms mainly dissolve in the interstitial sites of the β phase. The other is the hardening induced by the increased shear modulus of β phase after hydrogenation [15].

4. Conclusions

The effects of hydrogen content on the microstructural evolution, flow behaviour and work hardening of Ti–6Al–4V alloy deformed in β phase field were investigated, and the mechanism of hydrogen-induced hardening was discussed. Following conclusions were drawn from the present work:

(1) Hydrogen could be retained in Ti–6Al–4V alloy even though the temperature was increased to 1100 °C in air. δ hydride with an FCC crystal structure existed in the deformed matrix of the hydrogenated specimens. The size of δ hydride reduced when the deformation temperature was increased from 1050 to 1100 °C.
(2) The flow stress of Ti–6Al–4V alloy increased gradually with hydrogen at the strain rate of 1 s^{-1}. At the strain rate of 0.005 s^{-1}, however, hydrogen had little effect on the flow stress. Hydrogen showed a reduced effect on the increment of flow stress at 1100 °C compared to that at 1050 °C. The flow curves presented more significant oscillations at the strain rate of 1 s^{-1} relative to that at lower strain rate.
(3) Hydrogen induced increased work hardening rate of Ti–6Al–4V alloy when the alloy was deformed in β phase field. The work hardening rate showed an increasing trend with strain rate under the same hydrogen content level.
(4) Hydrogen had a positive effect on the development of twinning in Ti–6Al–4V alloy. Hydrogen-induced twinning played a key role in the occurring of work hardening of Ti–6Al–4V alloy in β phase field.

References

[1] Singh BK, Singh V. Effect of fast neutron irradiation on tensile properties of AISI 304 stainless steel and alloy Ti–6Al–4V. Mater Sci Eng A 2011;528:5336–70.
[2] Sun Y, Zeng W, Han Y, Ma X, Zhao Y, Guo P, et al. Determination of the influence of processing parameters on the mechanical properties of the Ti–6Al–4V alloy using an artificial neural network. Comput Mater Sci 2012;60:239–44.
[3] Momeni A, Abbasi SM. Effect of hot working on flow behavior of Ti–6Al–4V alloy in single and two phase regions. Mater Des 2010;31:3599–604.

[4] Giuliano G. Constitutive equation for superplastic Ti–6Al–4V alloy. Mater Des 2008;29:1330–3.
[5] Semiatin SL, Goetz RL, Shell EB, Seetharaman V, Ghosh AK. Cavitation and failure during hot forging of Ti–6Al–4V. Metall Mater Trans A 1999;30A:1411–24.
[6] Guan RG, Je YT, Zhao ZY, Lee CS. Effect of microstructure on deformation behaviour of Ti–6Al–4V alloy during compression process. Mater Des 2012;36:796–803.
[7] Shan DB, Zong YY, Lv Y, Guo B. The effect of hydrogen on the strengthening and softening of Ti–6Al–4V alloy. Scr Mater 2008;58:449–52.
[8] Zhang S, Zhao L. Effect of hydrogen on the superplasticity and microstructure of Ti–6Al–4V alloy. J Alloys Comp 1995;218:233–6.
[9] Li MQ, Zhang WF. Effect of hydrogen on processing maps in isothermal compression of Ti–6Al–4V titanium alloy. Mater Sci Eng A 2009;502:32–7.
[10] Lu J, Qin J, Lu W, Chen Y, Zhang Z, Zhang D, et al. Superplastic deformation of hydrogenated Ti–6A–4V alloys. Mater Sci Eng A 2010;527:4875–80.
[11] Kim JH, Semiatin SL, Lee CS. Constitutive analysis of the high-temperature deformation mechanisms of Ti–6Al–4V and Ti–6.85Al–1.6V alloys. Mater Sci Eng A 2005;394:366–75.
[12] Seshacharyulu T, Medeiros SC, Frazier WG, Prasad YVRK. Microstructural mechanisms during hot working of commercial grade Ti–6Al–4V with lamellar starting structure. Mater Sci Eng A 2002;325:112–25.
[13] Senkov ON, Jonas JJ. Effect of phase composition and hydrogen level on the deformation behavior of titanium–hydrogen alloys. Metall Mater Trans A 1996;27A:1869–76.
[14] He WJ, Zhang SH, Song HW, Cheng M. Hydrogen-induced hardening and softening of a β-titanium alloy. Scr Mater 2009;61:16–9.
[15] Senkov ON, Froes FH. Thermohydrogen processing of titanium alloys. Int J Hydrogen Energy 1999;24:565–76.
[16] Zhao J. Influence of thermo hydrogen treatment on microstructural evolution and high temperature deformation behavior of titanium alloys. Shenyang: Northeastern University; 2009.
[17] Bragg WH, Bragg WL. The reflection of X-rays by crystals. Proc Royal Soc London Ser A, Containing Pap Math Phys Charact 1913;88:428–38.
[18] Park CH, Ko YG, Park JW, Lee CS. Enhanced superplasticity utilizing dynamic globularization of Ti–6Al–4V alloy. Mater Sci Eng A 2008;496:150–8.
[19] Kocks UF, Mecking H. Physics and phenomenology of strain hardening: the FCC case. Prog Mater Sci 2003;48:171–273.
[20] Zhu Y, Zeng W, Zhao Y, Shu Y, Zhang X. Effect of processing parameters on hot deformation behaviour and microstructural evolution during hot compression of Ti40 titanium alloy. Mater Sci Eng A 2012;552:384–91.
[21] Zhao JW, Ding H, Hou HL, Li ZQ. Influence of hydrogen content on hot deformation behavior and microstructural evolution of Ti600 alloy. J Alloys Comp 2010;491:673–8.
[22] Puschl W. The flow stress contribution of the dislocation 'forest' in bcc lattices. Philos Mag Lett 2000;80:199–203.
[23] Hwang C, Bernstein IM. Hydrogen induced slip and twinning in iron alloys. Scr Metall 1982;16:85–90.
[24] Liu X, Su Y, Luo L, Liu J, Guo J, Fu H. Effect of hydrogen on hot deformation behaviors of TiAl alloys. Int J Hydrogen Energy 2010;35:13322–8.
[25] Gao KW, Nakamura M. Hydrogen embrittlement of Ti–49Al at various strain rates. Intermetallics 2002;10:233–8.
[26] Zong YY, Shan DB, Lu Y, Guo B. Effect of 0.3 wt% H addition on the high temperature deformation behaviors of Ti–6Al–4V alloy. Int J Hydrogen Energy 2007;32:3936–40.
[27] Wert JJ, Singerman SA, Caldwell SG, Quarles RA. The role of stacking fault energy and induced residual stresses on the sliding wear of aluminium bronze. Wear 1983;91:253–67.
[28] Salem AA, Kalidindi SR, Doherty RD, Semiatin SL. Strain hardening due to deformation twinning in α-titanium: mechanisms. Metall Mater Trans A 2006;37A:259–68.
[29] Salem AA, Kalidindi SR, Doherty RD. Strain hardening of titanium: role of deformation twinning. Acta Mater 2003;51:4225–37.